Journal of
Polymer & Composites
https://journals.stmjournals.com/jopc

ISSN: 2321-2810 (Online)
ISSN: 2321-8525 (Print)
Volume 14, Special Issue 1, 2026
DOI (Journal): 10.37591/JoPC

Research JoPC

# Modeling and Simulation of Radiative MHD Casson-Type Polymer Composite Flow over a Porous Wedge with Variable Thermal Source and Sink

B. Tulsi Lakshmi Devi[1], Alfunsa Prathiba[2,*], V.V.L. Deepthi[3], Sridevi Dandu[4]

**Abstract**

*This study presents a numerical investigation of the radiative magnetohydrodynamic (MHD) flow and heat transfer characteristics of a Casson-type polymer fluid over a moving and extending porous wedge under the influence of a spatially varying heat source and sink. The Casson fluid model, representing a class of viscoplastic polymeric materials, is analyzed within the MHD framework to explore the combined effects of magnetic field intensity, rheological behavior, and porous medium interaction on the transport characteristics. The governing nonlinear momentum and energy equations are transformed into a system of ordinary differential equations through similarity transformations and solved using the Runge–Kutta fourth-order method coupled with a shooting technique. The influence of key dimensionless parameters—including the magnetic parameter, Casson number, variable heat generation rate, and stretching velocity—on the velocity and temperature distributions is examined in detail. The results reveal that the magnetic field and Casson parameter significantly modify the boundary layer thickness and enhance heat transfer control. This investigation provides valuable insights into the thermo-rheological performance of MHD Casson polymer fluids in porous composite systems, with potential applications in polymer extrusion, composite material processing, and electronic cooling technologies.*

**Keywords:** Casson polymer fluid, MHD, porous wedge, radiative heat transfer, variable heat generation, polymer composites, numerical simulation.

## INTRODUCTION

***Author for Correspondence**
Alfunsa Prathiba

[1]Associate Professor, Department of Mathematics, Koneru Lakshmaiah Education Foundation, Hyderabad, Telangana, India
[2]Associate Professor, Department of Humanities and Sciences (Mathematics), CVR College of Engineering, Mangalpally, Ibrahimpatnam, Hyderabad, Telangana, India
[3]Sr. Assistant Professor, Department of Humanities and Sciences (Mathematics), CVR College of Engineering, Mangalpally, Ibrahimpatnam, Hyderabad, Telangana, India
[4]Assistant Professor, Department of Engineering Mathematics & Humanities, S.R.K.R. Engineering College, Bhimavaram, West Godavari District, Andhra Pradesh, India

Received Date: 06 November 2025
Accepted Date: 14 November 2025
Published Date: 04 December 2026

**Citation:** B. Tulsi Lakshmi Devi, Alfunsa Prathiba, V.V.L. Deepthi, Sridevi Dandu. Modeling and Simulation of Radiative MHD Casson-Type Polymer Composite Flow over a Porous Wedge with Variable Thermal Source and Sink. Journal of Polymer & Composites. 2026; 14(Special Issue 1): S837–S850p.

Polymers and their composites play a vital role in modern engineering and industrial applications due to their exceptional mechanical strength, lightweight nature, and superior thermal stability. They are widely utilized in thermal insulation systems, polymer extrusion, coating processes, biomedical devices, and electronic cooling technologies. The processing of polymeric materials often involves complex flow and heat transfer phenomena, particularly under the influence of magnetic fields, porous substrates, and varying thermal conditions. Understanding these thermo rheological characteristics is essential for optimizing material performance and ensuring stability in manufacturing and energy systems. Among the various configurations studied in heat transfer and fluid flow, wedge-shaped geometries have attracted considerable attention due to their wide applicability in polymer and composite processing, geothermal systems, heat exchangers, and thermal insulation. As noted by Nagendramma V. *et al*. [1] and Wubset Ibrahim and Ayele Tulu [2], wedge-based configurations are critical in analyzing heat transport mechanisms in practical systems. The impact of internal energy and stress on magnetohydrodynamic (MHD) convective flow over a wedge was first explored by Yih [3]. Earlier, Falkner and Skan [4] proposed the fundamental formulation for steady laminar flow past an isothermal wedge, effectively extending Prandtl's boundary layer theory. This work was further refined by Hartree [5] using similarity transformations, leading to numerical estimations of wall shear stress at different wedge angles. Subsequent studies [6-9] have expanded this analysis to include diverse physical effects, highlighting the importance of laminar boundary layer flow past wedge surfaces in both theoretical and applied contexts. Non-Newtonian fluid dynamics has emerged as a pivotal research area due to its extensive applications in industrial, biological, and engineering processes. Among the various non-Newtonian models, the Casson fluid model has gained significant prominence for its ability to represent fluids exhibiting yield stress behavior, including polymer solutions, suspensions, and biofluids. Alkasasbeh [10] conducted a numerical simulation of magnetohydrodynamic (MHD) radiative micropolar Casson fluid flow over a cylindrical surface, highlighting the influence of magnetic and thermal parameters on flow characteristics. Durgaprasad *et al*. [11] investigated the heat and mass transfer in a three-dimensional Casson nanofluid flow across a thin sheet embedded in a porous medium. Their study demonstrated that the thickness of the momentum and thermal boundary layers increased with higher Casson parameter values, emphasizing the rheological sensitivity of such fluids. Similarly, Anantha Kumar *et al*. [12] analyzed the unsteady MHD Casson flow with thermal radiation along a curved surface and statistically evaluated the associated heat transfer mechanisms. A considerable number of investigations have thus focused on Casson fluid behavior under diverse physical effects [13-18]. However, despite these advancements, significant challenges remain in understanding the combined influence of external magnetic fields, variable heat generation, and complex geometries such as wedge-shaped configurations, particularly when modeling polymer based Casson fluids in porous media. Addressing these gaps can provide valuable insight into the thermomechanical behavior of polymeric and composite fluid systems, which are essential in modern thermal management and polymer processing technologies. Recent developments in magnetohydrodynamic (MHD) and non-Newtonian fluid dynamics have substantially enhanced our understanding of heat and mass transfer phenomena in polymeric and composite fluid systems. Revathi *et al*. [20] investigated the influence of cross-diffusion, couple stress, and non-Fourier heat flux on Jeffrey hybrid nanofluid flow and entropy generation, emphasizing the significance of rheological complexity in thermal energy systems. Jyothi *et al*. [21] utilized neural network-based modeling to analyze MHD boundary-layer flow and heat transfer in Sisko nanofluids, reflecting the growing role of data-driven techniques in fluid mechanics. Bin Zafar *et al*. [22] explored Lorentz force effects on Prandtl-type two-phase nanomaterials containing microorganisms, demonstrating the coupling between magnetic fields and bioconvective behavior. Katikala *et al*. [23] examined Hall current, radiation absorption, and diffusion-thermo effects in unsteady MHD second-grade fluid flow through porous media, while Lavanya *et al*. [24] provided a comprehensive numerical study of Carreau nanofluid flow with Cattaneo–Christov heat flux to describe advanced heat conduction in polymeric systems. Similarly, Amjad Ali Pasha *et al*. [25] reported on rotational forces and thermal diffusion in viscoelastic MHD flows, and Ramachandra Reddy *et al*. [26] analyzed thermo-physical and aligned magnetic field effects on Casson fluids over inclined plates, extending understanding of MHD convection in viscoplastic systems. Hussain *et al*. [27] discussed the thermo-physical aspects of three-dimensional non-Newtonian hybrid nanofluids under rotational flow, while Valiveti *et al*. [28] analyzed unsteady MHD Casson fluid flow incorporating thermal diffusion and heat source effects. Prasad *et al*. [29] and Jyothi *et al*. [30] further explored Hall current, radiation, and chemical reaction effects in MHD nanofluid systems using neural network-assisted models, and Bhargava *et al*. [31] investigated 3D hybrid nanofluid flow through porous media under magnetic and radiative conditions, emphasizing the complexity of coupled thermal–electromagnetic phenomena in composite media. In the present study, a two-dimensional, steady, mixed convective magnetohydrodynamic (MHD) flow of a Casson-type polymer fluid past a moving wedge is investigated in the presence of a spatially varying heat source and sink. To the best of the authors' knowledge, no prior studies have reported this specific configuration combining Casson polymer fluid behavior, magnetic effects, and thermally active porous media. The governing partial differential equations representing the conservation of momentum and energy are transformed into a system of nonlinear ordinary differential equations using appropriate similarity transformations. These equations are then solved numerically using the Runge–Kutta fourth-order method in conjunction with the shooting technique. The influence of key dimensionless parameters—such as the magnetic field strength, Casson parameter, heat generation/absorption coefficient, and suction/injection velocity—on the velocity and temperature profiles is analyzed in detail. Furthermore, variations in the skin friction coefficient and Nusselt number are presented through comprehensive graphical and tabular representations for both suction and injection conditions. The obtained results contribute to a deeper understanding of the thermo-rheological characteristics of MHD Casson polymer fluids in porous wedge geometries, with potential implications for polymer extrusion, coating, and composite fabrication processes.

## PROBLEM FORMULATION

Consider a uniform mixed convective flow of a 2D MHD Casson fluid under the following assumptions:

1. The external magnetic field acted in the axial direction. The induced magnetic field created by the velocity of an electrically conducting fluid is overlooked, because it is relatively weak compared to the applied magnetic field.
2. $Uw$ is the stretching velocity of the wedge and U being the free stream velocity.
3. T and T∞ are the temperature at the wall of the wedge and the ambient temperature of the fluid, respectively. Figure 1 illustrates the selected coordinate system, with $x$ pointing parallel to the plate in the direction of the flow and $y$ pointing towards the free stream[2].

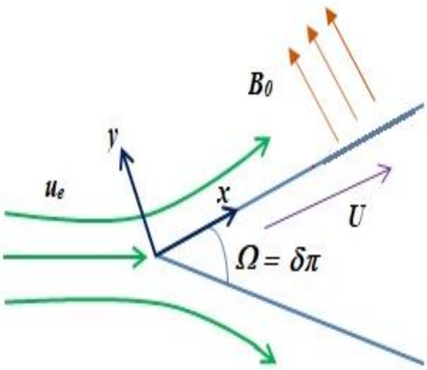


**Figure 1.** The problem's physical structure

Taking the above assumptions into account the boundary layer continuity, momentum and energy equations [19]are,

$$\frac{\partial u}{\partial x}+\frac{\partial u}{\partial y}=0 \tag{1}$$

$$u\frac{\partial u}{\partial x}+v\frac{\partial u}{\partial y}=U\frac{\partial U}{\partial x}+\nu\left(1+\frac{1}{\beta}\right)\frac{\partial^2 u}{\partial y^2}-\frac{\sigma {B_0}^2}{\rho}(u-U)+(T-T_\infty)g\beta_0 Sin\frac{\Omega}{2}, \tag{2}$$

$$\rho c_p\left(u\frac{\partial T}{\partial x}+v\frac{\partial T}{\partial y}\right)=-u\left(\rho U\frac{\partial U}{\partial x}+\sigma {B_0}^2 U\right)+\alpha\frac{\partial^2 T}{\partial y^2}$$
$$+\frac{kU}{x\nu}\left[A^*(T_w-T_\infty)\,exp\left(-y\sqrt{U}(\nu x)^{-1/2}\right)+B^*(T-T_\infty)\right]-\frac{\partial q_r}{\partial y} \tag{3}$$

The boundary conditions that are associated with the present problem are

$$T(x,y)=T_w, u(x,y)=U_w, v(x,0)=v_w, y\to 0, u(x,y)=U, T(x,y)=T_\infty asy\to\infty, \tag{4}$$

Where,

$$U=U_0x^m, U_w=RU, v_w=-C(\nu U_0)^{1/2}(m+1/2)x^{m-1/2}, T_w=T_\infty+bx^{2m}, \tag{5}$$

The radiation term using the "Rosseland approximation" is expressed by $\mathbf{q_r} = \frac{-4\sigma^*}{3k^*}\frac{\partial T^4}{\partial y}$(where $\boldsymbol{\sigma}^*$denotes Stefan-Boltzman constant, $\mathbf{k}^*$ absorption coefficient). Rewriting $\mathbf{T^4}$ using the Taylor's series expansion and escalating $\mathbf{T^4}$ about $\mathbf{T_\infty}$ and ignoring higher order terms takes

$T^4 = 4T_\infty^3 T - 3T_\infty^4$. We obtain $q_r = \frac{-16T_\infty^3\sigma^*}{3k^*}\frac{\partial T}{\partial y}$.

$$\eta = y\sqrt{U}(\nu x)^{-1/2}, \psi = U^{1/2}g(\eta)\sqrt{\nu x}, \theta(\eta) = \frac{T-T_\infty}{T_w-T_\infty}, \quad (6)$$

ψ is defined by

$$v = -\frac{\partial\psi}{\partial x}, u = \frac{\partial\psi}{\partial y} \quad (7)$$

Using the above Similarity transformations which satisfy the continuity equation, the equations (2) & (3) along with the boundary conditions are reduced to,

$$\left(1+\frac{1}{\beta}\right)g''' + \left(\frac{1+m}{2}\right)gg'' + m[1-(g')^2] - M(g'-1) + \left[\lambda\, Sin\frac{\Omega}{2}\right]\theta = 0, \quad (8)$$

$$(1+Rd)\frac{1}{\Pr}\theta'' + \left(\frac{1+m}{2}\right)g\theta' - 2m\theta g' - Ec\left[(m+M)g'\right] + A^*\exp(-\eta) + B^*\theta = 0 \quad (9)$$

These boundary conditions (4) are the ones that relate to them.

$$g'(\infty)=1, g'(0)=R, g(0)=C, \theta(0)=1, \theta(\infty)=0, \quad (10)$$

The prime symbol signifies the derivative with respect to η and the dimensionless flow governing parameters $M, Gr_x, \lambda, C, R, Ec$ and $\Pr$ are given by:

$$M = \frac{\sigma B_0^2}{\rho U_0}, Gr_x = \frac{g\beta_0(T_w - T_\infty)x^3}{\nu^2}, \mathrm{Re}_x = \frac{Ux}{\nu}, Ec = \frac{U^2}{c_p(T_w - T_\infty)},$$
$$\Pr = \frac{\mu c_p}{\alpha}, \lambda = \frac{Gr_x}{\mathrm{Re}_x^2}, Rd = \frac{16T_\infty^3\sigma_0}{3k^*\alpha}, R = Wedge\ stretching\ rate \quad (11)$$

**PHYSICAL QUANTITIES**

The coefficients of engineering interest such as Skin friction, Nusslet number are defined as

$$C_f = \frac{\tau_w}{\rho U^2}, \text{ where } \tau_w = \left(\mu_B + \frac{p_y}{\sqrt{2\pi}}\right)\left(\frac{\partial u}{\partial y}\right)_{y=0} \text{ and } Nu_x = \frac{xq_w}{\alpha(T_w - T_\infty)} \text{ where } q_w = -\alpha\left(\frac{\partial T}{\partial y}\right)_{y=0}.$$

Finally, in the non-dimensional form the above equations are given as follows:

$$\mathrm{Re}_x^{1/2} C_f = \left(1+\frac{1}{\beta}\right)g''(0) \text{ and } \mathrm{Re}_x^{-1/2} Nu = -\theta'(0). \quad (12)$$

**SOLUTION OF THE PROBLEM**

The reduced Eqs. (8) – (9) are highly nonlinear and coupled in nature, and thus, their closed form solutions are not possible. They can be solved numerically using Runge–Kutta-4 (RK-4) with shooting method for different values of parameters. The proposed RK-4 method with shooting technique is not new method, but it has been used extensively by several researchers in dealing with the problems of boundary layer flows. Furthermore, when compared to alternative approaches, the shooting technique used is efficient and produces great precision. That is why we used this method. In this work, we have used MATLAB software to simulate the flow. The study examines how the developing parameters affect the temperature, skin friction, dimensionless velocity, and Nusselt number. The step size is taken$\Delta\eta = 0.001$, and accuracy is up to the fifth decimal place as the criterion of convergence. We assumed a suitable finite value for the far-field boundary condition in (10), i.e.$\eta \rightarrow \infty$, say $\eta_\infty$. The inner iteration is done with the convergence criterion of $10^{-6}$ in all cases.

## RESULT AND DISCUSSION

The equations (8) & (9) along with (10) are numerically computed and the impact of the parameters such as $M, Gr_x, \lambda, C, R,$ Ec and $P_r$ on the velocity, temperature profiles are discussed below. Results of $Re^{1/2}C_f$ are compared with the numerical results obtained. It is noted that the achieved results have a wonderful agreement with each other and hereafter authenticate our solution method. Which is shown in table 1.

Figures 2 -12 are sketched to explain the aftermaths of miscellaneous parameters on fascinating fields. Figure 2 is sketched to see the effects of Casson fluid parameter $\beta$ when R = 1.5 i-e wedge stretches faster and R = 0.5 means wedge stretches slower. It is noted that for R < 1 as increases the velocity increases but for R > 1 it shows opposite behaviour. Figure 3 is prepared to see the effect of M when R > 1or R < 1. The $g'(\eta)$ declines with enhancement in values M when with the rise in M values the $g'(\eta)$ profiles decrease, whereas for R = 0.5, we have the reverse behavior. Moreover, various values of mixed convection parameters for R < 1 or R > 1 give the velocity variation as observed from Fig. 4. For assisting flow velocity increases for both the values of R but for opposing flow, the fluid velocity declines for both the values of R. Suction/injection parameter C effects are displayed in Fig. 5. For R = 0.5 and with the escalation in C the fluid velocity rises but for R = 1.5 it decreases.

The impact of $\beta$ on $\theta(\eta)$ is sketched in Fig. 6, and it is noted that a rise in leads to a decline in $\theta(\eta)$ for R = 1⁄2. Opposite behaviour occurs for R=1.5. However, temperature profiles exhibit a decreasing behaviour with an increase in R. Suction/injection parameter C effects are displayed in Fig. 7. For both values of R the escalation in C the fluid temperature declines. The impact of different parameters such as $\lambda$, Rd and Ec on temperature and velocity profiles shown in Figs. 8 - 10. It is noted that the increase in Ec or $\lambda$ results in a decrease in temperature profile, whereas the impact of the Rd parameter is found to be the opposite. Moreover, various values of heat generation or absorption parameters for R < 0.5 or R > 1 give the temperature variation as observed from Figs. 11 and 12. It is noted that the increase in $A^*$ or $B^*$ results in a increase in temperature profile.

Table 2 is made to see the influence of physical parameters on $Re^{-0.5}C_f$ for R < 1 and R > 1. When $\beta, m, M, C$ are slow R > 1 a rise in the value decreases skin friction and when the R < 1 we found an opposite behaviour. For both R<1 and R>1, the skin friction decreases for increasing values of Ec and $B^*$, whereas the skin friction increases for higher impact of Rd and$A^*$.

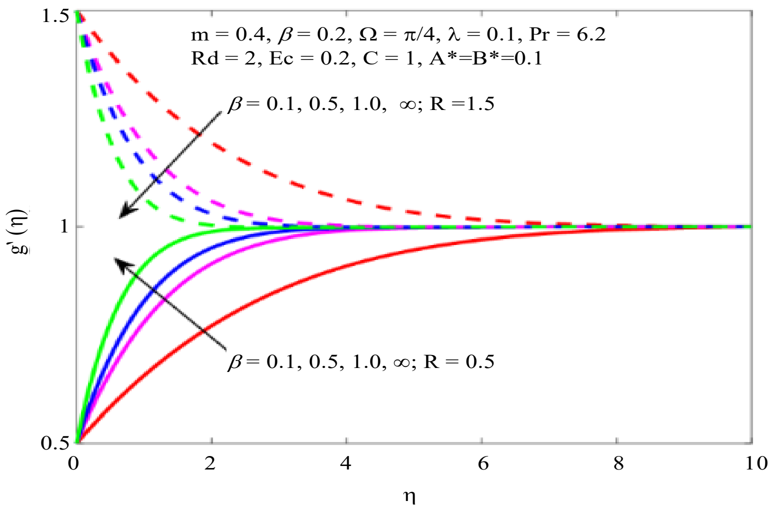


**Figure 2.** Velocity $g'(\eta)$ for different

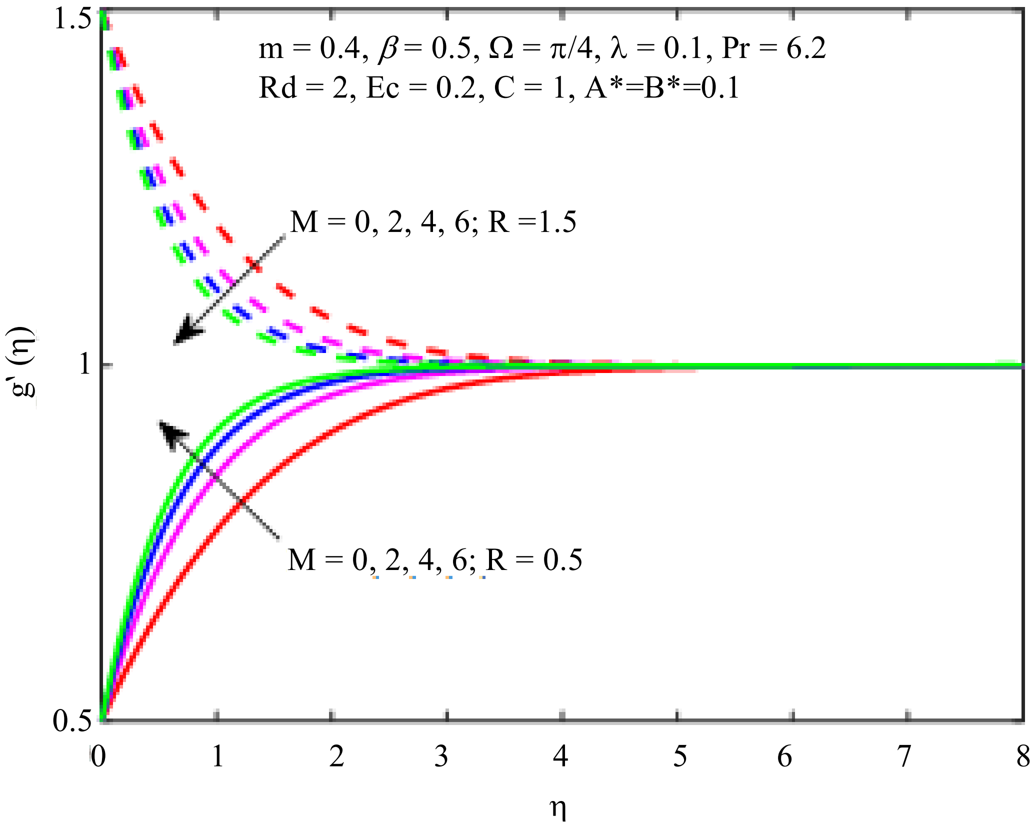


**Figure 3.** Velocity g′(η) for different M

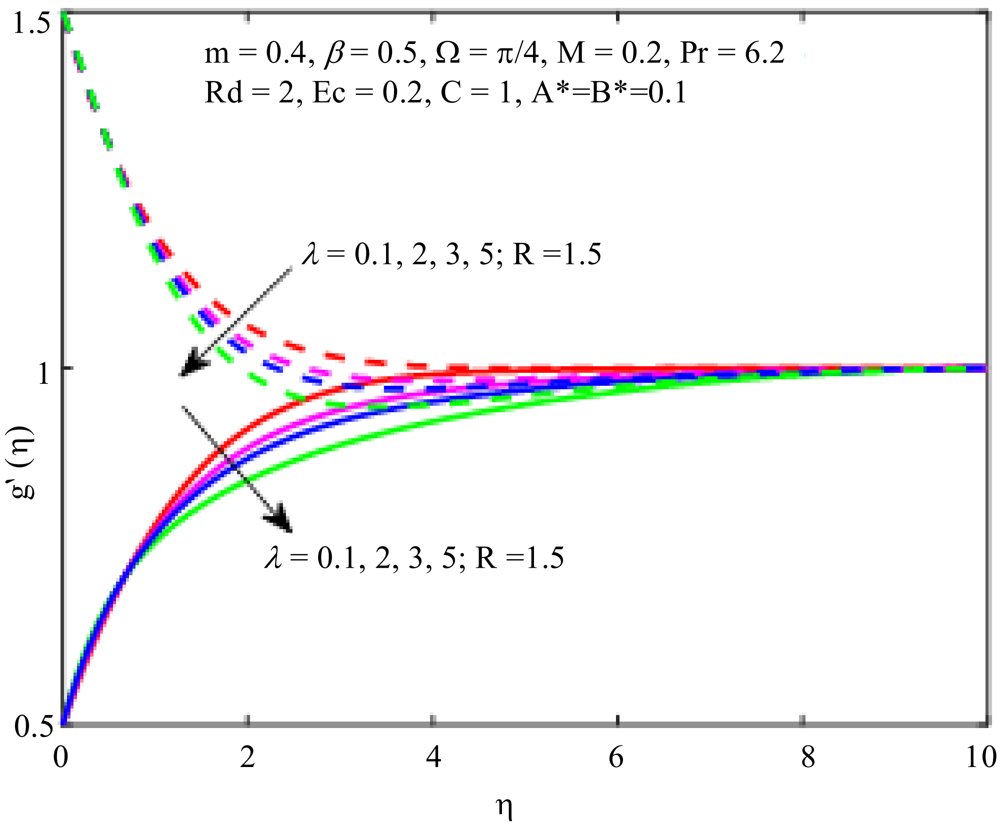

Journal of Polymer & Composites
Volume 14, Special Issue 1
ISSN: 2321-2810 (Online), ISSN: 2321-8525 (Print)

**Figure 4.** Velocity $g'(\eta)$ for different $\lambda$.

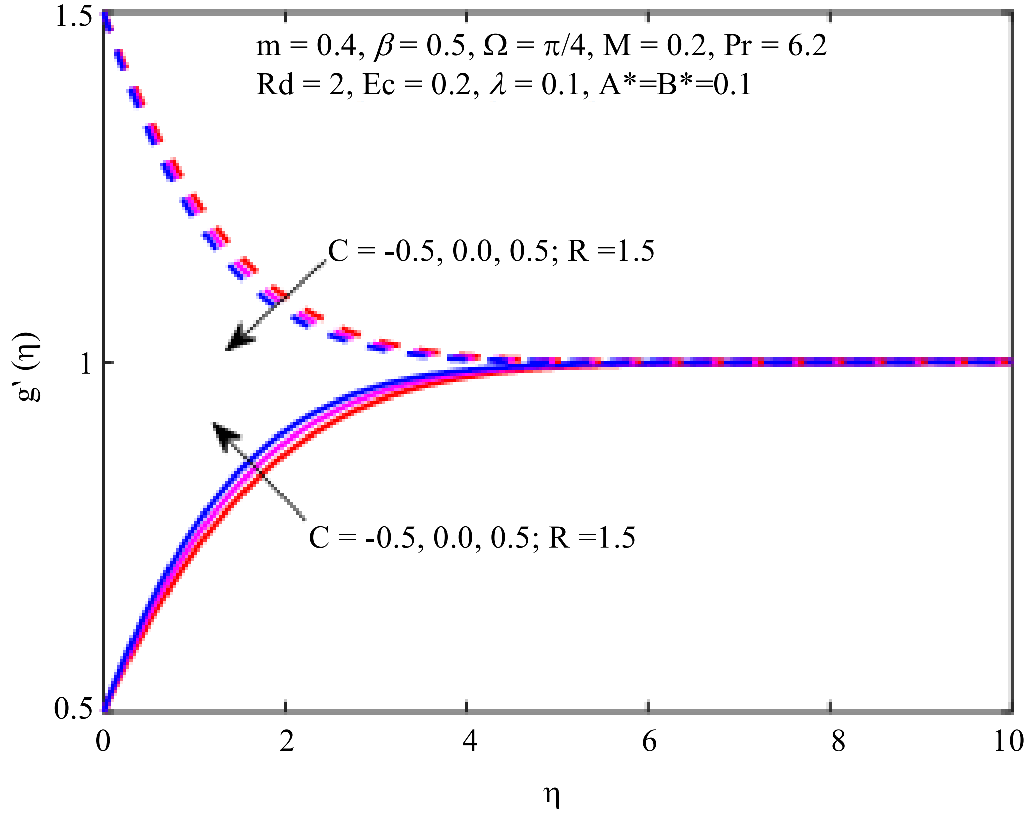


**Figure 5.** Velocity $g'(\eta)$ for different C

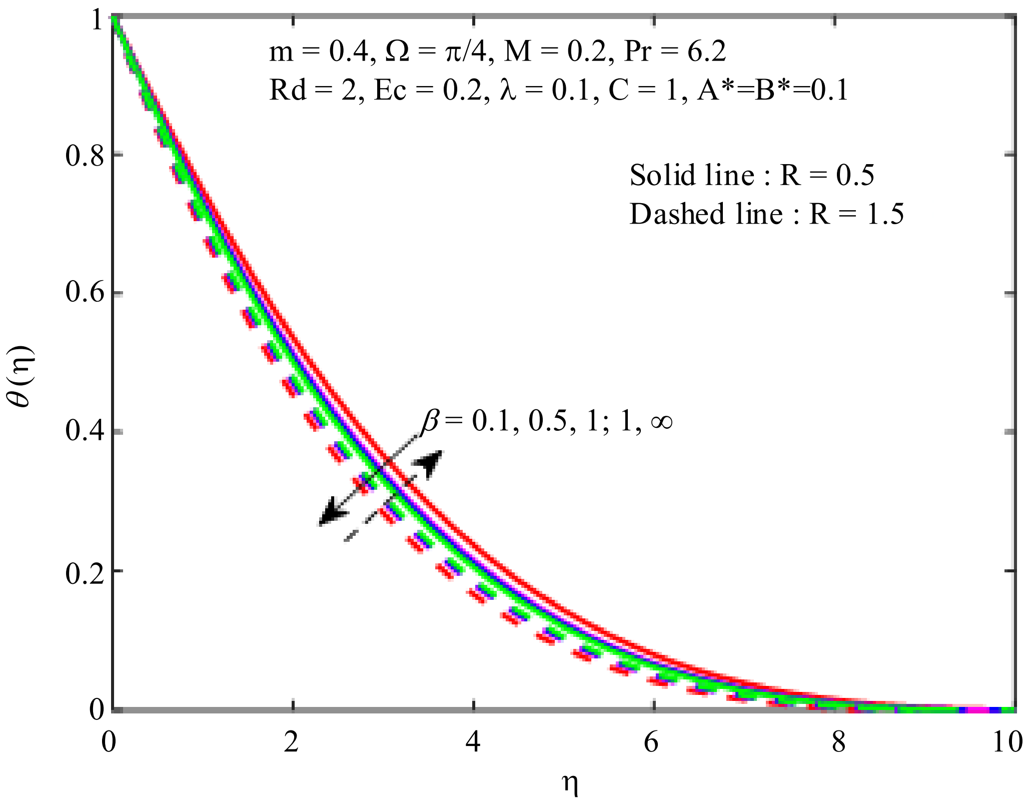


 

**Figure 6.** Temperature θ(η) for different β.

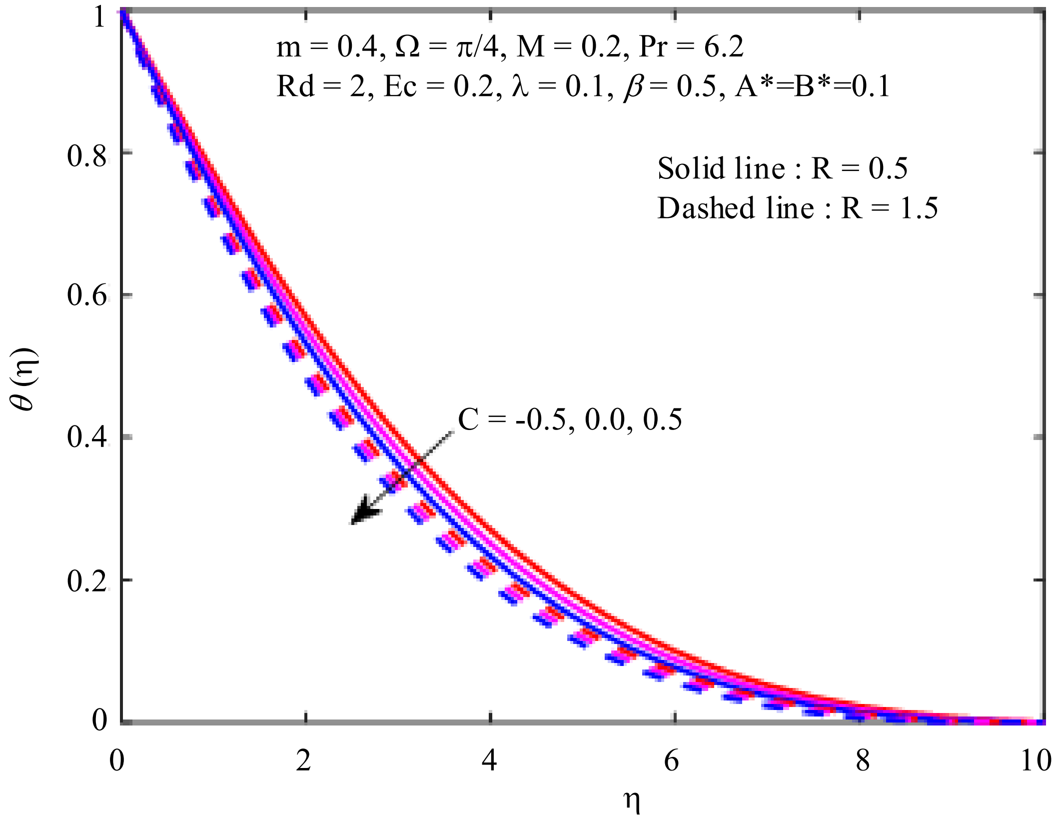


**Figure 7.** Temperature θ(η) for different C.

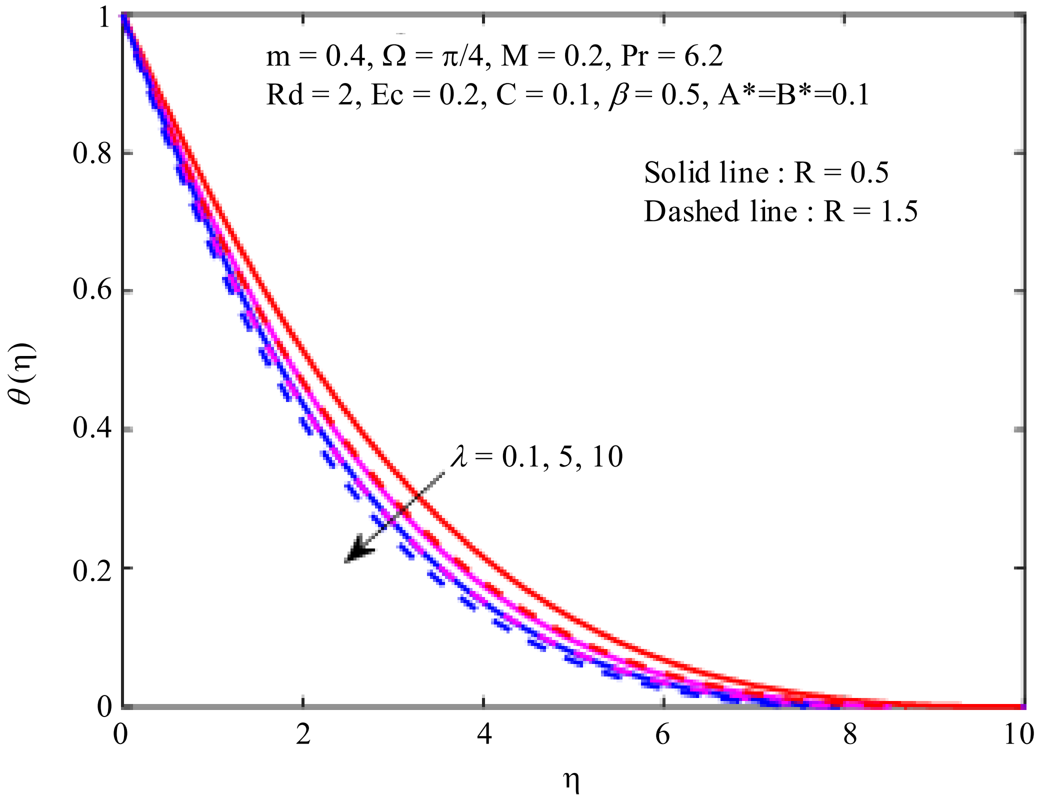


 

**Figure 8.** Temperature θ(η) for different λ.

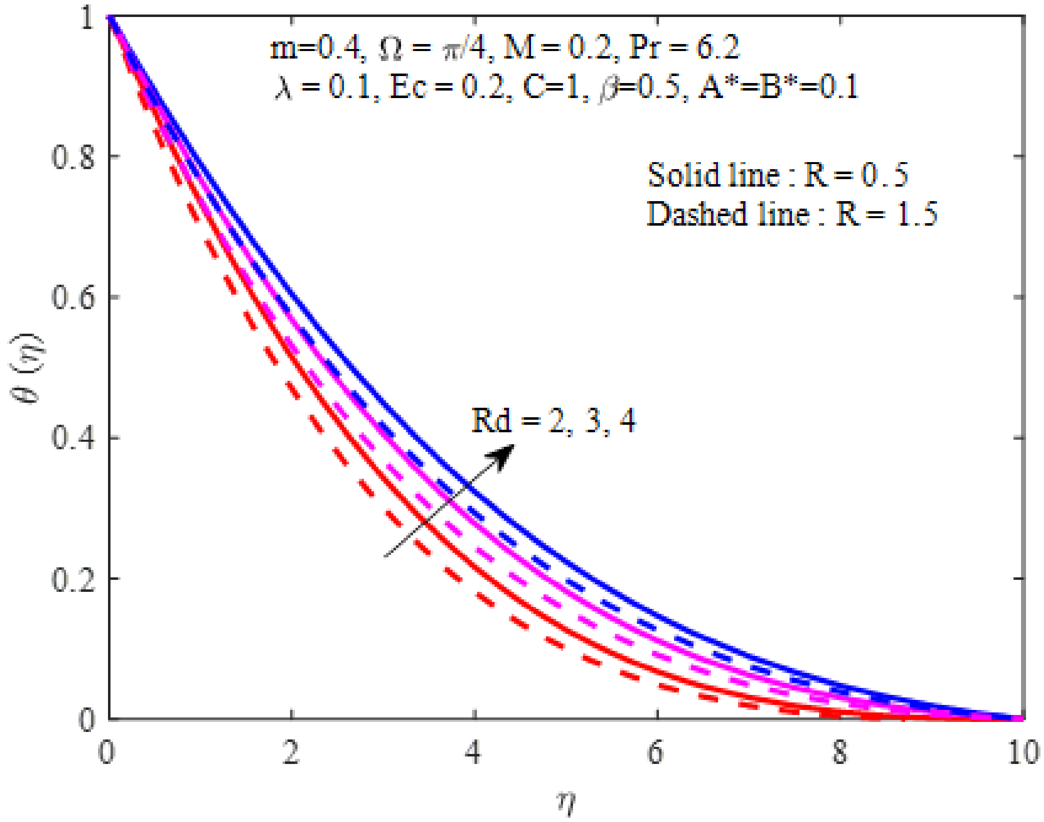


**Figure 9.** Temperature θ(η) for different Rd

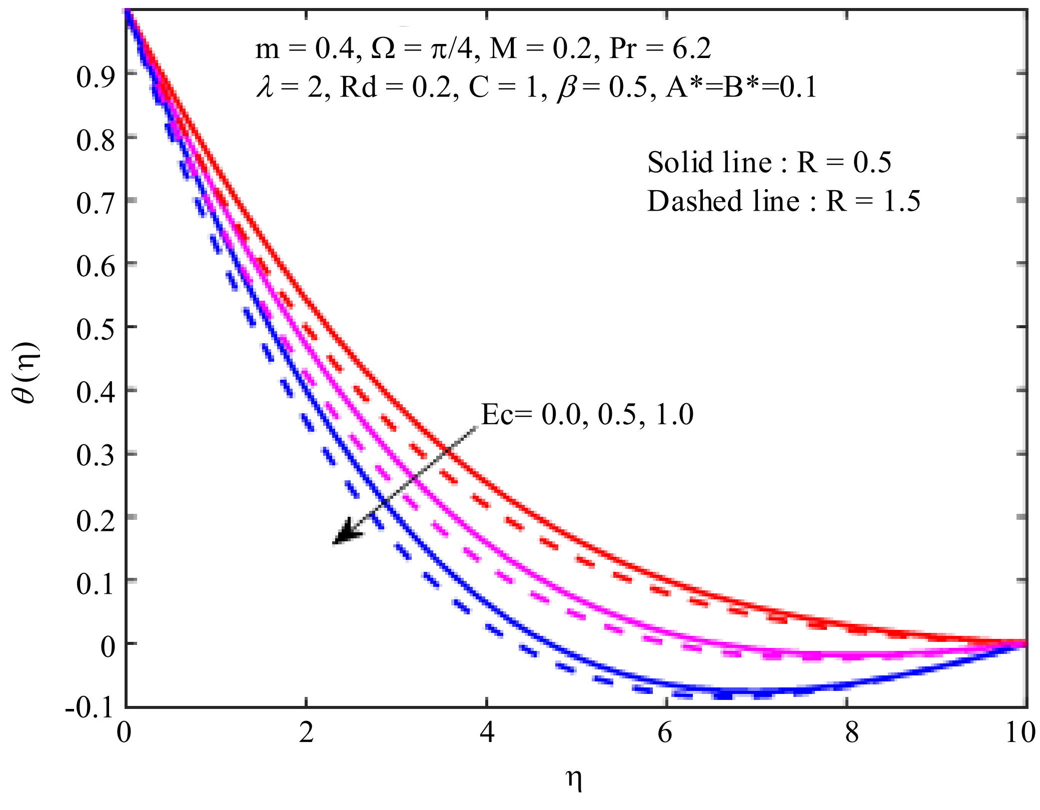

**Figure 10.** Temperature θ(η) for different values of Ec

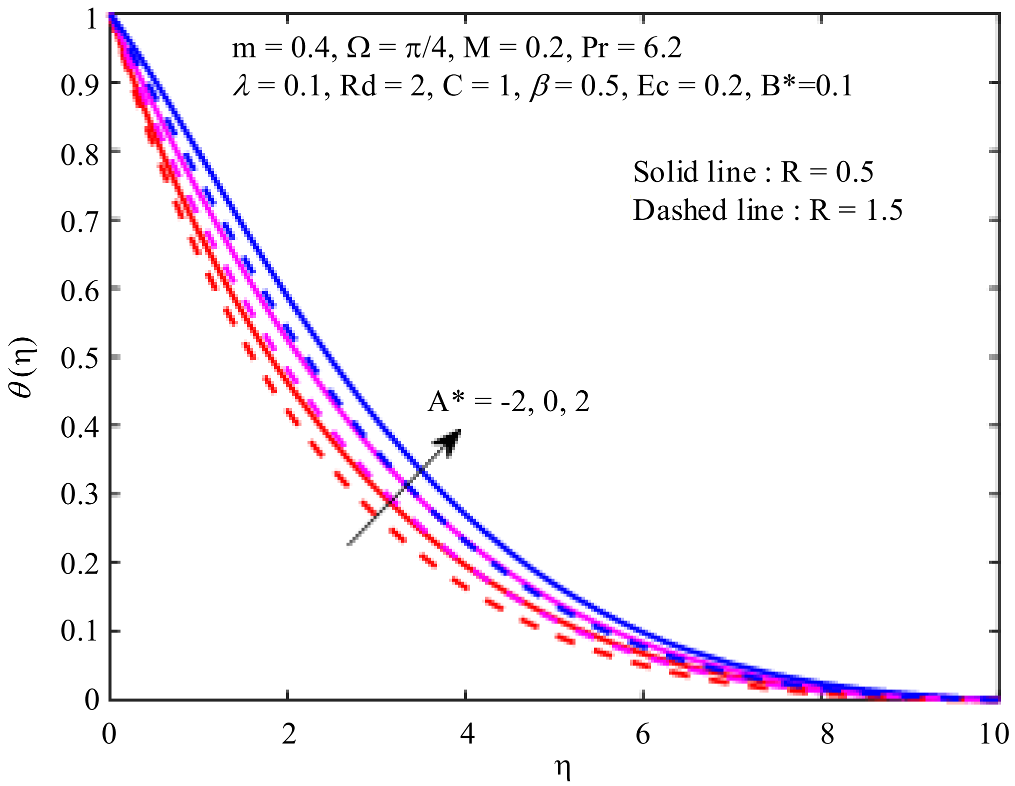


**Figure 11.** Temperature θ(η) for differentA*.

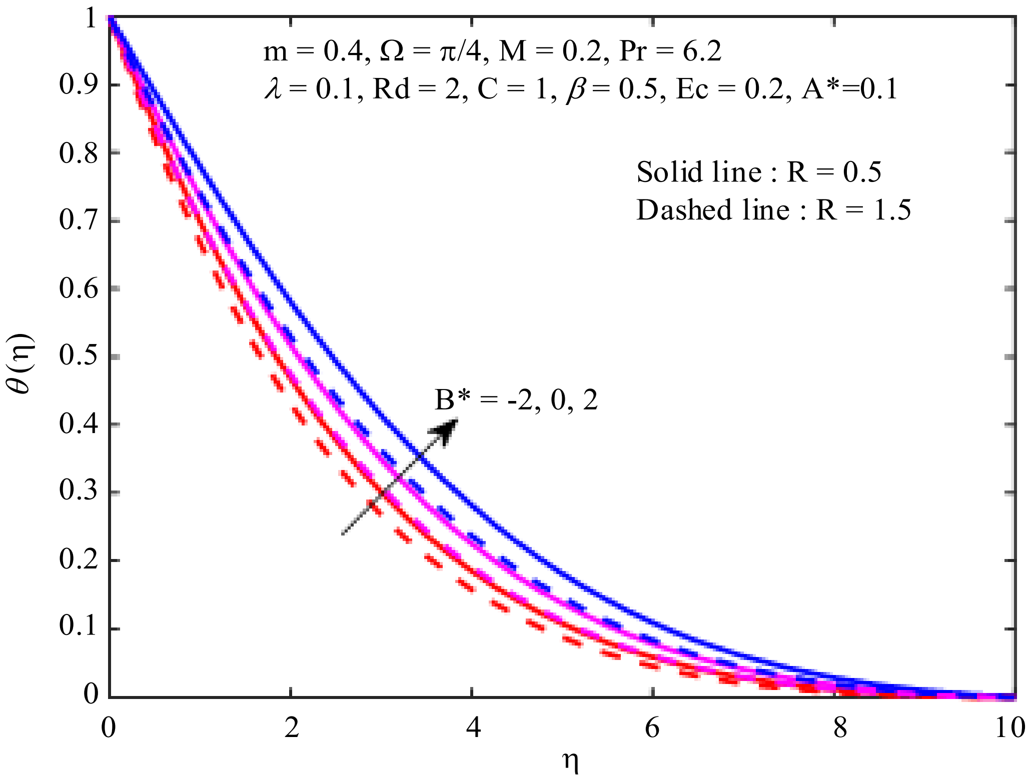


**Figure 12.** Effect of E on φ(n)

ISSN: 2321-2810 (Online), ISSN: 2321-8525 (Print)

**Table 1.** Comparison of $f''(0)$ with previous studies for various values of C, and when β=∞, m = 1, R = 0 = M.

| C | Ibrahim & Ayele[2] | Yih [3] | Present results |
|---|---|---|---|
| 1.0 | 1.8893 | 1.88931 | 1.889362 |
| -1.0 | 0.7566 | 0.75658 | 0.756535 |
| -0.5 | 0.9692 | 0.96923 | 0.969212 |
| 0.0 | 1.2326 | 1.23259 | 1.232235 |
| 0.5 | 1.5418 | 1.54175 | 1.541596 |

**Table 2.** Computation of $\mathrm{Re}_x^{1/2}\, Cf_x$, $\mathrm{Re}_x^{-1/2}\, Nu_x$ *and* $\mathrm{Re}_x^{-1/2}\, Sh_x$ for different parameters

| β | $m$ | M | C | Ec | Rd | A* | B* | $Re_x^{1/2}\, Cf_x$ | | $Re_x^{-1/2}\, Nu_x$ | |
|---|---|---|---|---|---|---|---|---|---|---|---|
| | | | | | | | | $R = 0.5$ | $R = 1.5$ | $R = 0.5$ | $R = 1.5$ |
| 0.5 | 0.4 | 0.2 | 1 | 0.2 | 2 | 0.1 | 0.1 | 0.380201 | -0.437619 | 2.248461 | 2.894157 |
| 1.0 | | | | | | | | 0.487548 | -0.555500 | 2.268094 | 2.883153 |
| 1.5 | | | | | | | | 0.546768 | -0.619848 | 2.278027 | 2.877217 |
| 20 | | | | | | | | 0.584721 | -0.660862 | 2.284086 | 2.873486 |
| | 0.8 | | | | | | | 0.485701 | -0.561150 | 3.001422 | 3.873378 |
| | 1.2 | | | | | | | 0.576191 | -0.665812 | 3.663222 | 4.707266 |
| | 1.6 | | | | | | | 0.657580 | -0.759235 | 4.277656 | 5.463999 |
| | 2.0 | | | | | | | 0.732731 | -0.844994 | 4.862079 | 6.171098 |
| | | 0.6 | | | | | | 0.427462 | -0.477596 | 2.291163 | 2.837272 |
| | | 1.0 | | | | | | 0.469613 | -0.514408 | 2.329442 | 2.784471 |
| | | 1.4 | | | | | | 0.507982 | -0.548673 | 2.364426 | 2.734984 |
| | | 1.8 | | | | | | 0.543414 | -0.580837 | 2.396834 | 2.688250 |
| | | | -1 | | | | | 0.253973 | -0.305999 | 0.515154 | 1.167588 |
| | | | -0.5 | | | | | 0.281473 | -0.335788 | 0.790365 | 1.492481 |
| | | | 0 | | | | | 0.311693 | -0.367724 | 1.180363 | 1.893542 |
| | | | 0.5 | | | | | 0.344642 | -0.401703 | 1.674296 | 2.364313 |
| | | | 1 | | | | | 0.380201 | -0.437619 | 2.248461 | 2.894157 |
| | | | | 0.6 | | | | 0.376236 | -0.440890 | 2.721554 | 3.378525 |
| | | | | 1.0 | | | | 0.372254 | -0.444171 | 3.195376 | 3.863697 |
| | | | | 1.4 | | | | 0.368254 | -0.447463 | 3.669935 | 4.349676 |
| | | | | 1.8 | | | | 0.364237 | -0.450767 | 4.145234 | 4.836468 |
| | | | | | 3 | | | 0.381040 | -0.436981 | 1.825247 | 2.375341 |
| | | | | | 4 | | | 0.381742 | -0.436436 | 1.561982 | 2.044869 |
| | | | | | 5 | | | 0.382346 | -0.435957 | 1.380452 | 1.812959 |
| | | | | | 6 | | | 0.382876 | -0.435529 | 1.246633 | 1.639678 |
| | | | | | | -0.5 | | 0.378312 | -0.438895 | 2.981349 | 3.512975 |
| | | | | | | -0.3 | | 0.378942 | -0.438470 | 2.737001 | 3.306683 |
| | | | | | | 0 | | 0.379886 | -0.437832 | 2.370576 | 2.997281 |
| | | | | | | 0.3 | | 0.380830 | -0.437194 | 2.004269 | 2.687922 |
| | | | | | | 0.5 | | 0.381458 | -0.436769 | 1.760128 | 2.481705 |
| | | | | | | | -0.5 | 0.380383 | -0.437385 | 2.541240 | 3.112796 |
| | | | | | | | -0.3 | 0.380355 | -0.437438 | 2.443721 | 3.038444 |
| | | | | | | | 0 | 0.380257 | -0.437562 | 2.296648 | 2.929216 |
| | | | | | | | 0.3 | 0.380035 | -0.437768 | 2.156247 | 2.827798 |
| | | | | | | | 0.5 | 0.379765 | -0.437975 | 2.075543 | 2.769492 |

## CONCLUSION

This study is to examine the 4th order R-K method on the thermal boundary layer flow over an extending wedge. The wedge is considered to be absorptive with the existence of Ohmic heating, thermal radiation and space dependent heat generation or absorption. From the figures and tables, we conclude the main investigations as follows:

- An increase in M reduces the momentum boundary layer thickness as R < 1 or R >1.
- As R → 1, g^' (η)has the highest value and the boundary layer is thin.
- g^' (η) velocity and θ(η) boundary layer width reduce with the rise of R.
- Skin friction for R < 1 decreases as it increases. However, it increases for R > 1 as we increased.
- When both R < 1 or R>1, the Nusselt number decreases as we increase the values of A^*or B^*.
- The skin friction enhances but Nusselt number decline as Rd upsurges.

## REFERENCES


1. Nagendramma V, Sreelakshmi K, and Sarojamma G, "MHD Heat and Mass Transfer Flow over a Stretching Wedge with Convective Boundary Condition and Thermophoresis," *Procedia Eng*., vol. 127, pp. 963–969, 2015, doi: 10.1016/j.proeng.2015.11.444.
2. W. Ibrahim and A. Tulu, "Magnetohydrodynamic (MHD) Boundary Layer Flow Past a Wedge with Heat Transfer and Viscous Effects of Nanofluid Embedded in Porous Media," *Math. Probl. Eng*., vol. 2019, no. 1, Jan. 2019, doi: 10.1155/2019/4507852.
3. K. A. Yih, "MHD forced convection flow adjacent to a non-isothermal wedge," *Int. Commun. Heat Mass Transf.,* vol. 26, no. 6, pp. 819–827, Aug. 1999, doi: 10.1016/S0735-1933(99)00070-6.
4. V. M. Falkneb and S. W. Skan, "Some approximate solutions of boundary layer equations," *Philos. Mag. J. Sci*., vol. 12, no. 80, pp. 865–896, Nov. 1931, doi: 10.1080/14786443109461870.
5. D. R. Hartree, "On an equation occurring in Falkner and Skan's approximate treatment of the equations of the boundary layer," *Math. Proc. Cambridge Philos. Soc.,* vol. 33, no. 2, pp. 223–239, Apr. 1937, doi: 10.1017/s0305004100019575.
6. B. S. Goud, y. D. Reddy, and adnan, "numerical investigation of the dynamics of magnetized casson fluid flow over a permeable wedge subject to dissipation and thermal radiations," *Surf. Rev. Lett*., vol. 31, no. 07, Jul. 2024, doi: 10.1142/S0218625X24500549.
7. Shiva Rao and P. Deka, "a numerical study on heat transfer for mhd flow of radiative casson nanofluid over a porous stretching sheet," *Lat. Am. Appl. Res. - An Int. J*., vol. 53, no. 2, pp. 129–136, Feb. 2023, doi: 10.52292/j.laar.2023.950.
8. C. Sulochana and M. Poornima, "Unsteady MHD Casson fluid flow through vertical plate in the presence of Hall current," SN Appl. Sci., vol. 1, no. 12, p. 1626, Dec. 2019, doi: 10.1007/s42452-019-1656-0.
9. E. U. Haq *et al*., "Author Correction: Numerical aspects of thermo migrated radiative nanofluid flow towards a moving wedge with combined magnetic force and porous medium," *Sci. Rep*., vol. 12, no. 1, p. 12034, Jul. 2022, doi: 10.1038/s41598-022-16367-0.
10. H. T. Alkasasbeh, "Numerical solution on heat transfer magnetohydrodynamic flow of micropolar casson fluid over a horizontal circular cylinder with thermal radiation," *Front. Heat Mass Transf*., vol. 10, Apr. 2018, doi: 10.5098/hmt.10.32.
11. P. Durgaprasad, S. V. K. Varma, M. M. Hoque, and C. S. K. Raju, "Combined effects of Brownian motion and thermophoresis parameters on three-dimensional (3D) Casson nanofluid flow across the porous layers slendering sheet in a suspension of graphene nanoparticles," *Neural Comput. Appl*., vol. 31, no. 10, pp. 6275–6286, Oct. 2019, doi: 10.1007/s00521-018-3451-z.
12. K. Anantha Kumar, V. Sugunamma, and N. Sandeep, "Effect of thermal radiation on MHD Casson fluid flow over an exponentially stretching curved sheet," *J. Therm. Anal. Calorim*., vol. 140, no. 5, pp. 2377–2385, Jun. 2020, doi: 10.1007/s10973-019-08977-0.
13. M. G. Reddy, "Thermal radiation and chemical reaction effects on MHD mixed convective boundary layer slip flow in a porous medium with heat source and Ohmic heating," *Eur. Phys. J. Plus*, vol. 129, no. 3, pp. 1–17, 2014, doi: 10.1140/epjp/i2014-14041-3.


 

14. M. I. Khan, M. Waqas, T. Hayat, and A. Alsaedi, "A comparative study of Casson fluid with homogeneous-heterogeneous reactions," *J. Colloid Int*erface *Sci*., vol. 498, pp. 85–90, 2017, doi: 10.1016/j.jcis.2017.03.024.
15. W. Alghamdi *et al*., "Boundary layer stagnation point flow of the Casson hybrid nanofluid over an unsteady stretching surface," *AIP Adv*., vol. 11, no. 1, 2021, doi: 10.1063/5.0036232.
16. S. Zahir, "Magnetohydrodynamic CNTs Casson Nanofluid and Radiative heat transfer in a Rotating Channels," *J. Phys. Res. Appl*., vol. 1, no. 1, pp. 017–032, 2018, doi: 10.29328/journal.jpra.1001002.
17. S. M. Mousavi, M. N. Rostami, M. Yousefi, S. Dinarvand, I. Pop, and M. A. Sheremet, "Dual solutions for Casson hybrid nanofluid flow due to a stretching/shrinking sheet: A new combination of theoretical and experimental models," *Chinese J. Phys*., vol. 71, pp. 574–588, Jun. 2021, doi: 10.1016/J.CJPH.2021.04.004.
18. A. Prathiba and A. V. Lakshimi, "Exploration of the Internal Energy Effect on 3D-Casson Fluid Embedded by Porous Media over A Rotating Sheet," *European Journal of Mathematics and Statistics,* vol. 3, no. 3, pp. 1–12, 2022, doi: http://dx.doi.org/10.24018/ejmath.2022.3.3.111.
19. N. Amar and N. Kishan, "The influence of radiation on MHD boundary layer flow past a nano fluid wedge embedded in porous media," *Partial Differ. Equations Appl. Math*., vol. 4, p. 100082, Dec. 2021, doi: 10.1016/j.padiff.2021.100082.
20. G. Revathi, M.S. Upadhya, K. Raghunath, Yadav, D., Kommaddi, H., & Jayachandra Babu, M., Influence of cross-diffusion, couple stress, and non-Fourier heat flux on Jeffrey hybrid nanofluid flow and entropy generation in a vertical cylinder. Phase Transitions, 2025, 1–22. https://doi.org/10.1080/01411594.2025.2536187
21. K. Jyothi, B. Venkateswarlu, P. Chandra Reddy, K. Raghunath, A. Damodara Reddy, Neural network-driven analysis of MHD boundary layer flow and heat transfer in Sisko nanofluids. Multiscale and Multidiscip. Model. Exp. and Des. **8**, 291 (2025). https://doi.org/10.1007/s41939-025-00877-1
22. S.S. Bin Zafar, A. Zaib, F. Ali, K. Raghunath, Nehad Ali Sh, Computational analysis of Lorentz force on Prandtl two phase nanomaterial involving microorganism due to stretching Cylinder. Z Angew Math Mech. 105, e70076 (2025). https://doi.org/10.1002/zamm.70076
23. Katikala N. V. Ch Bhargava, Shaik Mohammed Ibrahim, Raghunath Kodi, Effects of hall current, radiation absorption and diffusion thermo on an unsteady MHD flow of second grade fluid through porous media in the presence of joule heating and viscous dissipation. *Multiscale and Multidiscip. Model. Exp. and Des.* **8**, 260 (2025). https://doi.org/10.1007/s41939-025-00842-y
24. B. Lavanya, J. Girish Kumar, K. Raghunath, Y. Rameswara Reddy, M. Jayachandra Babu, A comprehensive study of Carreau nanofluid flow over an inclined vertical plate with Cattaneo-Christov heat flux: numerical simulation and statistical analysis. Radiation Effects and Defects in Solids, 2025, 1–18. https://doi.org/10.1080/10420150.2025.2484722
25. Amjad Ali Pasha, Mohammed K. Al Mesfer, M.W Kareem, K. Raghunath, M. Danish, S. Patil, V. Ramachandra Reddy, Effects of rotational forces, and thermal diffusion on unsteady magnetohydrodynamic (MHD) flow of a viscoelastic fluid through porous media with isothermal inclined plates, Case Studies in Thermal Engineering, Volume 69, 2025, 105977. https://doi.org/10.1016/j.csite.2025.105977.
26. V. Ramachandra Reddy, K. Raghunath, P. Imran Khan, K. Sudhakaru, Thermo-physical and aligned magnetic field effects on unsteady MHD convection in Casson fluids over isothermal inclined plates in the presence of joule heating and viscous dissipation, Thermal Advances, Volume 3, 2025, 100030. https://doi.org/10.1016/j.thradv.2025.100030.
27. S. Hussain, V.V.L**.** Deepthi, V. Omeshwar Reddy, K. Raghunath, L. Giulio, Thermo physical aspects of three dimensional non-newtonian Fe3O4/Al2O3 water based hybrid nanofluid with rotational flow over a stretched plate. International Journal of Heat and Technology, Vol. 43, No. 1, 2025, pp. 67-75. https://doi.org/10.18280/ijht.430108
28. S. Valiveti, M. Jetti, M. R. Yallalla, R. Kodi, and G. Lorenzini, "Analysis of heat and mass transfer in unsteady magnetohydrodynamic MHD Casson fluid flow over isothermal inclined plates with

thermal diffusion and heat source effects," Power Eng. Eng. Thermophys., vol. 3, no. 3, pp. 195–208, 2024. https://doi.org/10.56578/peet030305

29. V. R. Prasad, N.U.B. Varma, B. Jamuna, M.S. Suresh, K. Sudhakaru, K. Raghunath, Effects of hall current and thermal diffusion on unsteady MHD rotating flow of water based Cu, and TiO2 nanofluid in the presence of thermal radiation and chemical reaction. *Multiscale and Multidiscip. Model. Exp. and Des.* **8**, 161 (2025). https://doi.org/10.1007/s41939-025-00736-z
30. K. Jyothi, A. Sailakumari, V. Ramachandra reddy, K. Raghunath, Neural network-assisted analysis of MHD boundary layer flow and thermal radiation effects on SWCNT nanofluids with Maxwellian and non-Maxwellian models. *Multiscale and Multidiscip. Model. Exp. and Des.* **8**, 155 (2025). https://doi.org/10.1007/s41939-025-00752-z
31. K.N.V.C. Bhargava, S.M. Ibrahim, K. Raghunath, Magneto-hydrodynamic mixed convection chemically rotating and radiating 3D hybrid nanofluid flow through porous media over a stretched surface. Mathematical Modelling and Numerical Simulation with Applications, 4(4), 2024, 495-513. https://doi.org/10.53391/mmnsa.1438636

 